Communication

Coupling of Liquid Crystals to Silica Nanoparticles

Vincent Rachet, Khalid Lahlil, Mathieu Brard, Thierry Gacoin, and Jean-Pierre Boilot

J. Am. Chem. Soc., **2007**, 129 (30), 9274-9275• DOI: 10.1021/ja0735608 • Publication Date (Web): 11 July 2007

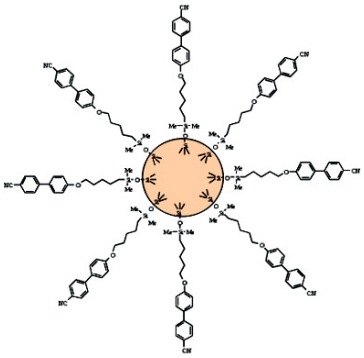

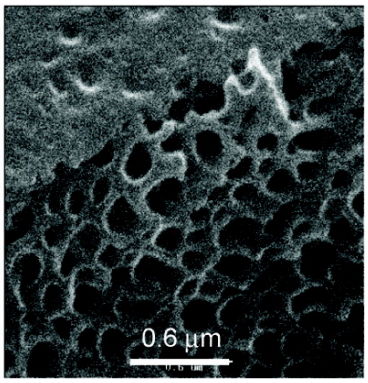

More About This Article

Additional resources and features associated with this article are available within the HTML version:

- Supporting Information
- Links to the 1 articles that cite this article, as of the time of this article download
- Access to high resolution figures
- Links to articles and content related to this article
- Copyright permission to reproduce figures and/or text from this article

View the Full Text HTML

J|A|C|S
COMMUNICATIONS

Published on Web 07/11/2007

Coupling of Liquid Crystals to Silica Nanoparticles

Vincent Rachet, Khalid Lahlil, Mathieu Bérard, Thierry Gacoin, and Jean-Pierre Boilot*

Laboratoire de Physique de la Matière Condensée, Ecole Polytechnique, CNRS, 91128 Palaiseau, France

Received May 18, 2007; E-mail: jean-pierre.boilot@polytechnique.fr

Electro-optical properties of polymer-dispersed liquid crystal (PDLC)[1,2] or holographic polymer-dispersed liquid crystal (H-PDLC)[3−7] are strongly related to optical index contrast between polymer matrix and electro-optical nematic phase. In PDLC, orientation of liquid crystal clusters located in droplets is controlled by an external electric field which allows matching the liquid crystal (LC) and polymer refractive indexes. When LC droplet diameters are in a range of a micrometer, devices switch from light scattering to transparent states providing indices are matched. Reducing the size of liquid crystal droplets to the sub-wavelength scale leads to nonscattering films, with a remaining electro-optic coefficient and a polarization insensitivity for a normally incident wave.

These kinds of biphasic structures are usually obtained by photoinduced phase separation (PIPS). Starting from a homogeneous mixture of monomer and LC molecules, a curing process induces a phase separation and formation of LC droplets. It is commonly accepted that the phase separation is usually not complete and that a part of LC molecules remains trapped in the polymer matrix.[8,9] This kinetics effect is largely amplified for nanometric droplets (50−100 nm) which only contain a small LC volume fraction, increasing the driving voltage for PDLC, decreasing the spatial modulation of the optical index, and leading to low diffraction efficiency for H-PDLC recordings. The partial phase separation and resulting morphologies have been recently explained using a general Onsager theory of transport, highlighted the role of the initial nucleation phase, and suggested the use of nucleation centers to control the LC volume fraction in droplets.[10]

In this paper, specific centers are prepared from the covalent grafting of cyano-biphenyl LC molecules at the surface of silica nanoparticles, allowing perfect stability of these particles into the nematic phase. The grafting rate is precisely determined by ^{1}H NMR, with a simple and original procedure used for the first time to quantify the functionalization of inorganic oxide particles. Finally, in a preliminary study, LC-functionalized silica nanoparticles are used as nucleation centers in a PIPS process with thiol-ene monomers and cyano-biphenyl LC molecules. A large enhancement of the phase separation is then observed from SEM observations with a complete demixtion where all the initial LC molecules go within the LC droplet volume. This should obviously increase the refractive index spatial modulation and improve electro-optic properties, especially the response time, in nanosized PDLC devices.

We designed and synthesized vinyl-substituted **L1** and ethoxy-dimethylsilane-substituted **L2** LC molecules as shown in Chart 1. In preliminary experiments, acid-catalyzed hydrolysis and condensation reactions of **L2** were followed in THF by ^{1}H NMR, using an internal reference constituted of a capillary tube filled of a p-xylene solution in $CDCl_3$. It was observed that the time evolution of monomer and dimer species can be easily quantified from chemical shift and intensity changes of the NMR peaks assigned to methyl groups coupled to the silicon atom. The hydrolysis rate was also deduced from the integration of the methylene triplet signal due to the ethanol formation.

Chart 1. Structures of LC Molecules ($n = 4-9$) for Grafting on Silica Particles

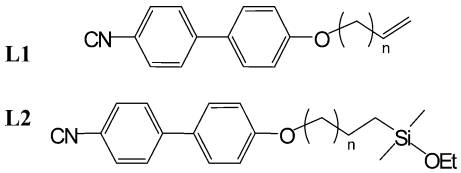

The same method of characterization was performed to follow the covalent grafting reaction of **L2** molecules at the surface of silica nanoparticles. A commercial suspension of silica nanoparticles in methanol was used (Nissan, MA-ST type, 14 nm in diameter). After solvent transfer and evaporation of methanol, 162.5 mg of silica in 1 ml of DMF were mixed to different quantities (from 18 to 64 mg) of **L2** in a sealed NMR tube. The mixture was refluxed for a few hundred of hours and ^{1}H NMR spectra were periodically recorded. As observed for pure **L2** molecules, the concentrations of starting monomer, hydrolyzed monomer, and dimer compounds can be easily deduced from ^{1}H NMR liquid spectra in the 0.40−0.50 ppm chemical shift range (Figure 1, left). When time is increased, the total concentration of these molecular species progressively decreases to a plateau, corresponding to the progressive grafting of **L2** molecules at the surface of silica nanoparticles. During ^{1}H liquid NMR sequences, protons belonging to **L2** molecules coupled to nanoparticles do not have sufficient time to relax and are not detected. Consequently, the study of the decrease of NMR signals assigned to molecular species allows calculation of the fraction of grafted **L2** molecules on silica particles, resulting from condensation reactions between hydrolyzed monomers and silanol groups located at the surface of particles.

Figure 1 (right) shows the time evolution of the different **L2**-type species by using 57 mg (125.6 μmol) of LC molecules. After introduction of silica particles and as shown by recording the first NMR spectrum, monomers are rapidly hydrolyzed and it then appeared to be a competition between the dimerization of hydrolyzed monomers and their condensation with silanol groups at the

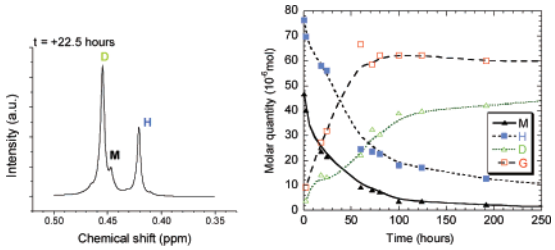

Figure 1. (Left) Typical ^{1}H liquid NMR spectrum observed during the coupling of **L2** LC molecules to silica nanoparticles in DMF. (Right) Time evolution of **L2** LC species. The concentration of LC molecules grafted on nanoparticles (G) was deduced from the decrease of the total intensity of ^{1}H liquid NMR peaks assigned to molecular monomers (M), hydrolyzed monomers (H), and dimer (D) species.

10.1021/ja0735608 CCC: $37.00

surface of particles. In these experiments, the condensation kinetics of LC molecules appears to be faster at the surface of particles. A simple simulation using a kinetics model previously developed by Pouxviel et al.[11] for hydrolysis−condensation reactions of sol−gel precursors indicates that the rate constant is about 5 times higher than that for the self-condensation of hydrolyzed **L2** monomers. In fact, **L2** monomers are preferentially hydrolyzed by confined water molecules located near the surface of hydrophilic silica particles, allowing rapid condensation of hydrolyzed monomers with surface silanol groups. After about 60 h in our experimental conditions, the grafting on particles is stopped while both hydrolysis and self-condensation reactions of **L2** monomers go on. This indicates a saturation of the surface of particles, and this is a clear check that the starting LC monomers are used in excess in these experiments. The saturation effect was also highlighted by observing the same plateau when increasing the initial concentration of **L2** monomers. The concentration of grafted silanol sites at the surface of nanoparticles can be easily deduced from these NMR experiments with an accurate precision of about 5%. The value is 0.38 ± 0.01 mmol·g^{-1}. Taking into account both experimental measurement of the density of silica nanoparticles (1.88 g·cm^{-3}) and of the average size of nanoparticles (14 ± 4 nm) deduced from microscopy observations, the grafting rate is ~1 LC molecule/nm^2 at the surface of nanoparticles. Assuming the presence of 4−6 OH/nm^2 at the surface of silica particles, as previously deduced from ignition measurements,[12] shows that, due to steric effects, only about 20% of the initial silanol groups are grafted by LC molecules. This is in agreement with previous values determined by other techniques (^{29}Si NMR and thermal analysis) for grafting experiments performed on the same type of silica particles.[13]

After elimination of remaining molecular species (see Supporting Information), the grafted particles can be dispersed at high concentration in organic solvents (20−25 wt% in dichloromethane and in the pure cyano-biphenyl LC), while starting silica nanoparticles are only soluble in polar solvents.

LC-grafted nanoparticles were tested in PIPS experiments to prepare PDLC with submicrometer sized droplets. PDLC samples were prepared from a standard thiol-ene polymerizable mixture belonging to the Norland series (NOA81, 70 wt %) with a typical nematic LC (BL24 from Merck, 30 wt %). Note that the densities of the monomer and LC are equal, allowing volume and weight fractions to be assimilated. Curing process was performed in cells (20 μm in thickness) under UV light (150 mW·cm^{-2}) for 4 min. One set of samples was initially doped with about 5 wt % of LC-grafted nanoparticles. After curing, cells were opened and metallized with a Au/Pd alloy for SEM observations. Assuming spherical droplets, the 3D size distribution can be computed from 2D SEM pictures (Figure 2), leading to the whole volume occupied by LC droplets. For samples without particles (Figure 2a), droplets (average size of 420 nm) only fill 14.8% of the total volume. This means that about 50% of the initial LC molecules are trapped into the polymer walls corresponding to a partial phase separation. Concerning the sample containing LC-grafted nanoparticles (Figure 2b), the microstructure is very different with a larger number of droplets of smaller sizes (average of 170 nm). In this case, the droplet volume is 28%, showing that the phase separation is complete with about all of the LC molecules in droplets. Another significant difference between the two types of samples is given by the optical

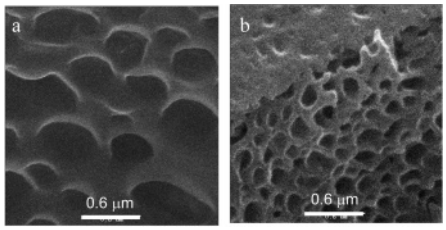

Figure 2. SEM images of typical PDLC samples obtained after curing a mixture of thiol-ene monomers and nematic LCs. (a) PDLC from a standard mixture without nanoparticles; (b) PDLC from a mixture containing LC-grafted silica nanoparticles as nucleation centers.

transmission. While the nondoped sample is quite transparent in the visible range, the doped one is white, indicating large diffusion efficiency in spite of a lower nanometric size of droplets (Figure S2). This suggests that light diffusion in the doped sample is drastically increased by a larger optical index mismatch.

These results clearly demonstrate that LC-grafted nanoparticles act as nucleation centers during the PIPS process leading to a complete phase separation and a premature stop of the growing process, which decreases the size of droplets. By reaching for the first time a complete separation between liquid crystal and polymer, LC-grafted nanoparticles offer new opportunities to the PDLC community, allowing better diffraction efficiency with thinner films, and then can advantageously decrease addressing voltage and response time of future H-PDLC components. Beyond the PDLC phase separation control, the ability to disperse silica particles at high concentrations in pure LC can lead to verification of theoretical predictions[14] and allow new devices to be created.

Acknowledgment. We are grateful to P. Le Barny and P. Feneyrou (Thales Research Technology) for fruitful discussions.

Supporting Information Available: Experimental details for the synthesis of **L1** and **L2** LC molecules, characterization of silica nanoparticles. This material is available free of charge via the Internet at http://pubs.acs.org.

References

(1) Bouteiller, L.; Le Barny, P. *Liq. Cryst.* **1996**, *21*, 157−174.
(2) Bouteiller, L.; Le Barny, P.; Martinot-Lagarde, Ph. *Liq. Cryst.* **1994**, *17*, 709−716.
(3) Qi, J.; De Sarkar, M.; Warren, G. T.; Crawford, G. *J. Appl. Phys.* **2002**, *91*, 4795−4800.
(4) Suntherland, R. L.; Tondiglia, V. P.; Natarajan, L. V.; Bunning, T. J. *Appl. Phys. Lett.* **2001**, *79*, 1420−1422.
(5) Suntherland, R. L. *J. Opt. Soc. Am.* **2002**, *19*, 2995−3012.
(6) Suntherland, R. L.; Tondiglia, V. P.; Natarajan, L. V.; Chandra, S.; Tomlin, D.; Bunning, T. J. *Opt. Express* **2002**, *10*, 1074−1082.
(7) Divlianski, I. S.; Mayer, T. S.; Holliday, K. S.; Crespi, V. H. *Appl. Phys. Lett.* **2003**, *82*, 1667−1669.
(8) Bunning, T. J.; Natarajan, L. V.; Tondiglia, V. P.; Sutherland, R. L.; Vezie, D. L.; Adams, W. W. *Polymer* **1995**, *36*, 2699−2708; **1996**, *37*, 3147−3150.
(9) Rachet, V.; Feneyrou, P.; Loiseaux, B.; Machke, U.; Le Barny, P.; Huignard, J. P. *Mol. Cryst. Liq. Cryst.* **2004**, *421*, 165−174.
(10) Rachet, V.; Feneyrou, P.; Le Barny, P.; Loiseaux, B.; Huignard, J. P. *Proc. SPIE* **2004**, *5518*, 211−219.
(11) Pouxviel, J. C.; Boilot, J. P.; Beloeil, J. C.; Lallemand, J. Y. *J. Non-Cryst. Solids* **1987**, *89*, 345−350.
(12) Iller, R. K. *The Chemistry of Silica*; Wiley-Interscience: New York, 1979.
(13) Douce, J.; Boilot, J. P.; Biteau, J.; Scodellaro, L.; Jimenez, A. *Thin Solid Films* **2004**, *1*−*2*, 114−122.
(14) (a) Poulin, P. *Science* **1997**, *275*, 1770−1773. (b) Mondain-Monval, O.; Poulin, P. *J. Phys.: Condens. Matter* **2004**, *16*, 1873−1885.

JA0735608